



Dependence of laser parameters on structural properties of pulsed laser-deposited MoS₂ thin films applicable for field effect transistors

Jianfeng Xi^{1,*} , Xiaowei Huang^{2,3}, Minghao Hu^{2,3}, and Wenfeng Xiang^{2,3}

¹Department of Physics, Beijing Technology and Business University, Beijing 100048, People's Republic of China

²Beijing Key Laboratory of Optical Detection Technology for Oil and Gas, China University of Petroleum, Beijing 102249, People's Republic of China

³College of New Energy and Materials, China University of Petroleum, Beijing 102249, People's Republic of China

Received: 26 March 2020

Accepted: 7 October 2020

Published online:
16 October 2020

© Springer Science+Business
Media, LLC, part of Springer
Nature 2020

ABSTRACT

The pulsed laser deposition (PLD) technique can be efficient and cost-effective in the fabrication of high-quality MoS₂ thin films. The laser pulse parameters, such as the number of pulses, the pulse energy density, and the frequency, that influence the MoS₂ thin films quality have been investigated. The optimum parameters of laser pulse for the best crystalline quality MoS₂ films were determined by experiments. Back-gated field effect transistors (FETs) were fabricated based on the MoS₂ thin film. The carrier mobility of the MoS₂ back-gated FETs has reached 4.63 cm² V⁻¹ S⁻¹. The responsivity of the MoS₂ back-gated FETs is approximately 0.06 AW⁻¹ at drain voltage of − 2 V. These results show that the back-gated FETs based on MoS₂ thin films prepared by PLD can be applied to photodetectors.

1 Introduction

Two-dimensional materials such as graphene, MoS₂, WS₂, MoSe₂, and GaSe have attracted tremendous technological and scientific interest in recent years due to their remarkable mechanical, electronic, and optical properties which are absent in their bulk counterparts [1–4]. Unlike graphene, the band gap of transition metal dichalcogenides (TMD) can be tuned from direct to indirect by simply varying the number of layers [5–7]. Nowadays, MoS₂, being one of the most intensively studied TMD materials, received

remarkable consideration. Owing to the extraordinary layer-dependent bandgap behavior, MoS₂ is considered a promising candidate to overcome the shortages belonging to zero-bandgap graphene, providing a possible solution for electronic applications, such as field effect transistors (FETs) [8], phototransistors [9], solar cells [10], and sensors [11]. In previous study, multilayer MoS₂ transistors were synthesized by a top-down growth technique, which showed a normally on accumulation mode characteristics with an electron mobility of > 80 cm²/Vs and an on/off ratio of > 10⁵ [12]. Flexible

Address correspondence to E-mail: xijf@btbu.edu.cn

photodetectors of MoS₂ were fabricated by chemical vapor deposition (CVD), and the responsivity is 570 A/W at 642 nm [13]. Monolayer and multilayer MoS₂ also can be produced by mechanical exfoliation with excellent quality, which have been successfully used for sensing NO gas [14].

Some of the fabrication methods reported for MoS₂ include laser thinning, CVD, mechanical exfoliation, lithium intercalation, liquid exfoliation, and chemical bath deposition. However, the lateral dimensions of films synthesized by these various methods have mostly been limited to the order of a few hundred microns [15]. At present, many practical applications of MoS₂ require the growth of large-area and high-quality compatible films to enable reliable and reproducible devices at a reasonable cost. In this way, how to control the area, geometry, size, and consistency among the number of layers is the key for the industrial application of MoS₂ thin films [16].

The pulsed laser deposition (PLD) technique has proven to be rapid, efficient, easy operation, and cost-effective in the fabrication of high-quality thin films [17]. In practical applications, it is well known that growth conditions have great influence on crystalline quality, microstructure, thickness, surface morphology, and mechanical properties of films [18]. Many works have reported the effects of pulse number, substrate, and substrate temperature on the characteristics of MoS₂ films. Ho et al. found that the number of grown MoS₂ layers can be effectively controlled by the pulse number of the excimer laser [19]. Barvat et al. have grown large-area continuous bilayer MoS₂ films by using the PLD technique on two different substrates, namely, sapphire and Si/SiO₂. The results revealed a homogeneous 2H-MoS₂ phase on sapphire and slightly sulfur deficient on Si/SiO₂ [20]. Serna et al. reported the deposition of MoS₂ layered films on SiO₂ and sapphire using the PLD technique. In their work, the effect of the substrate temperature was confirmed to improve the MoS₂ order quality, as well as the synthesis of layered material without a post-annealing treatment on amorphous SiO₂ and crystalline sapphire [21].

However, the investigations on the pulse parameters, such as pulse energy density and frequency, of MoS₂ films deposited by PLD technique are still little. In this work, the MoS₂ films were grown on sapphire and Si/SiO₂ substrates by PLD. Investigation on the evolution of surface morphology, thickness, and crystalline quality of MoS₂ films as a function of laser

pulse parameters was accomplished systematically. A detailed study of pulse frequency in MoS₂ films growth would be worthwhile and can provide useful information for a better understanding and improvement of the crystalline quality of the films and for the fabrication of MoS₂-based MEMS devices. Finally, we explored the transport characteristics and photoelectric response of the MoS₂-based FETs.

2 Experimental details

The MoS₂ thin films were deposited on sapphire substrates by using PLD method. The substrates were cleaned in ethanol and acetone by ultrasonication, each for 3 min, and then rinsed in deionized water, after which the films were dried by blowing N₂ gas on their surfaces. One piece of the cleaned substrates was then immediately loaded into a PLD chamber, and subsequently, the chamber was evacuated to a base pressure of 8×10^{-4} Torr. A commercially purchased MoS₂ (99.9% purity) target was mounted on a rotating target holder at a distance of ~ 10 cm from the substrates. The laser source was a pulsed KrF excimer laser operating at 248 nm. The substrate temperature was held at 700 °C. The pulses number was set at 400, 1200, 3600, and 7200, respectively. The range of pulse energy density was from 6.5 to 25.5 mJ/cm². The pulse frequency was precisely controlled and set at 2, 4, 6, 8, and 10 Hz. The deposition time of all films was approximately 2 min. After the film growth, the samples were cooled down to room temperature in growth pressure at a rate of 10 °C/min.

Ex situ growth characterization was performed by transmission electron microscopy (TEM), scanning electron microscopy (SEM), and Raman spectroscopy to study the thickness, surface morphology, and crystalline quality of the grown films. SEM images were captured with a 5.0 keV electron beam. The Raman spectra were recorded, with a (LabRAM HR) using Ar laser (532 nm) in the back-scattering geometry. Surface chemistry was studied by X-ray photoelectron spectroscopy (XPS). To construct the FETs structure, radio frequency magnetron sputtering technique was used to deposit Ag electrodes on surface of MoS₂ films and on the back side of SiO₂/Si substrates. The total deposition time of Ag electrodes was 10 min. The transport and transfer measurements were conducted in a semiconductor

characterization system. All the tests were executed at 300 K in atmosphere.

3 Results and discussions

3.1 Structural and chemical analysis of MoS₂ thin films

Figure 1 shows the TEM image of a few layer MoS₂ thin film deposited by PLD with 7200 laser pulses, pulse frequency of 6 Hz, and laser energy density of 25.5 mJ/cm². As shown in Fig. 1, the MoS₂ thin film exhibits different crystalline regions, which means that the MoS₂ film prepared by PLD is not monocrystal film. The sample of MoS₂ thin film was characterized by XPS to confirm the stoichiometry. Figure 2 shows the XPS spectra of the MoS₂ thin film deposited by PLD with 7200 laser pulses, pulse frequency of 6 Hz, and laser energy density of 25.5 mJ/cm². The chemical elements Mo, S, O, and C are detected by full spectrum scanning in the range of 0–1200 eV, as shown in Fig. 2a. As shown in Fig. 2b, C 1s peak is mainly derived from carbon in the air, and the binding energy is measured to be around 284.0 eV. The binding energies of O 1s are around 531.5 eV. The main sources of O 1s peak are oxygen in the air and oxides on the surface of the film. S is derived from the MoS₂ thin film, and the main pair of peaks in S 2p core level at 162.9 eV and 161.8 eV corresponds to S²⁻ 2p^{3/2} and S²⁻ 2p^{1/2}, as shown in Fig. 2c. In Fig. 2d, the peaks of Mo 3d located at 229.4 eV and 232.4 eV could be assigned to Mo 3d_{5/2} and Mo 3d_{3/2} of Mo⁴⁺ state in MoS₂, respectively.

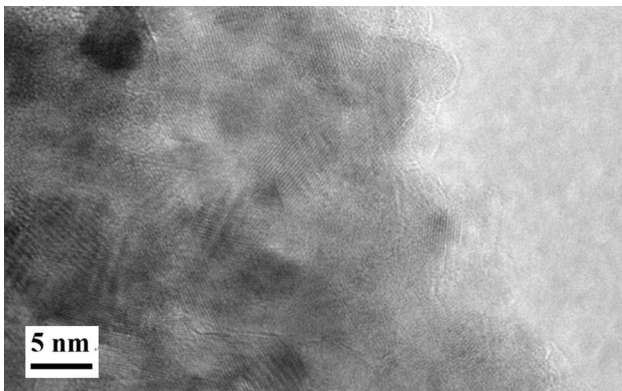


Fig. 1 TEM image of MoS₂ thin film deposited on an aluminum oxide substrates by PLD with 7200 pulses, pulse frequency of 6 Hz, and pulse energy density of 25.5 mJ/cm²

The XPS spectra indicates that the MoS₂ thin film is a thermodynamically stable 2H-MoS₂ semiconductor material rather than a metastable 1T-MoS₂ metal material [22]. Meanwhile, the Mo 3d core level peaks at 232.4 eV and 235.3 eV are attributed to the Mo⁶⁺ state of MoO₃. The stoichiometric components of MoS₂ film can be calculated based on the formula:

$$C_i = \frac{I_i/S_i}{\sum(I_j/S_j)}$$

where C_i is corresponding atomic concentration, I_i is corresponding atomic peak area, and S_i is corresponding atomic sensitivity factor. By the calculation, Mo to S ratio in the MoS₂ film is approximately two to three. Compared with stoichiometric ratio, 25% of sulfur atoms is missing. 19.2% of them were replaced by oxygen, the rest of 5.8% were sulfur vacancies. This result is consistent with the films deposited by using MoS₂ target [23].

3.2 Effect of pulses number on MoS₂ thin films

Figure 3 shows the SEM images of the films prepared with laser pulse energy of 25.5 mJ/cm², laser pulse frequency of 2 Hz, and different laser pulses. As shown in Fig. 3a, in the film deposited with 400 pulses, a large number of black dots can be seen. A continuous film was not deposited on the substrate, but a large number of nucleating points were seen because the pulses were too few. As the pulses number increased to 1200, the black spots on the surface disappear and white particles appear on the surface. The amount of white particles continues to increase with increasing number of pulses. At the same time, the particle size also increased, as shown in Fig. 3b–d. The typical size of the white particles is approximately 50–100 nm. These white particles on the surface have also appeared in other studies on the MoS₂ films prepared by PLD [24]. This is probably because some of the particles in the plume plasma fail to form films and gather on the surface of the film, which generate MoS₂ clusters during the deposition. With the increasing of deposition time, the number of particles increased, thus increasing the particle density of the film surface. Spherical particles of various dimensions are often seen in different PLD-deposited films, and the mechanisms of their formation are still under investigation [25].

Fig. 2 XPS spectra of MoS₂ film: **a** Survey, **b** O1s, **c** S2p, and **d** Mo3d

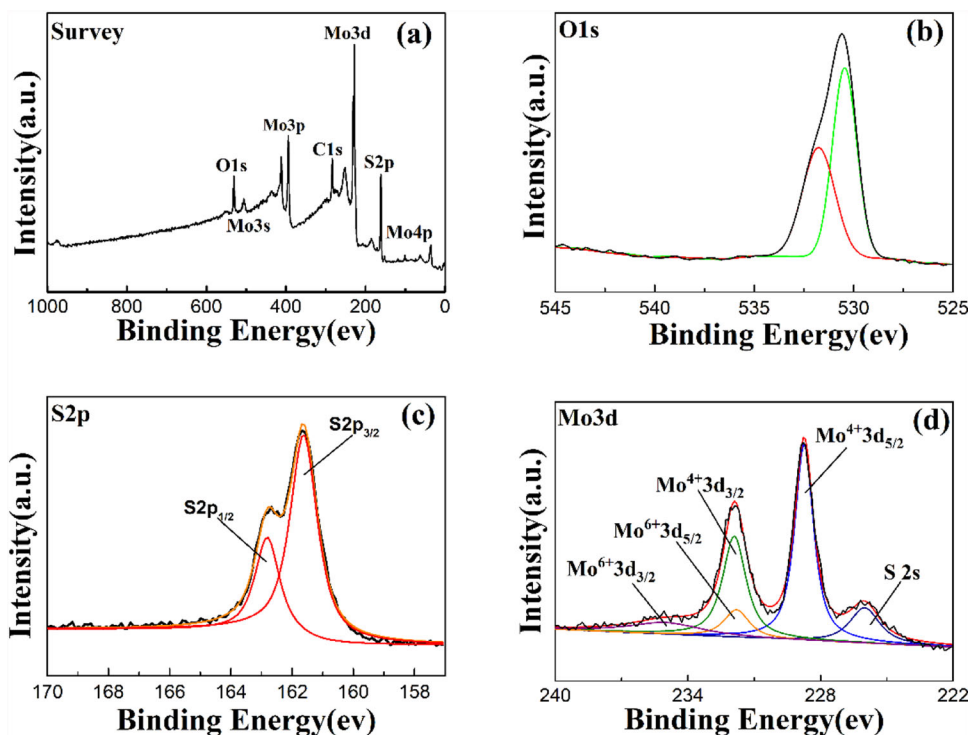
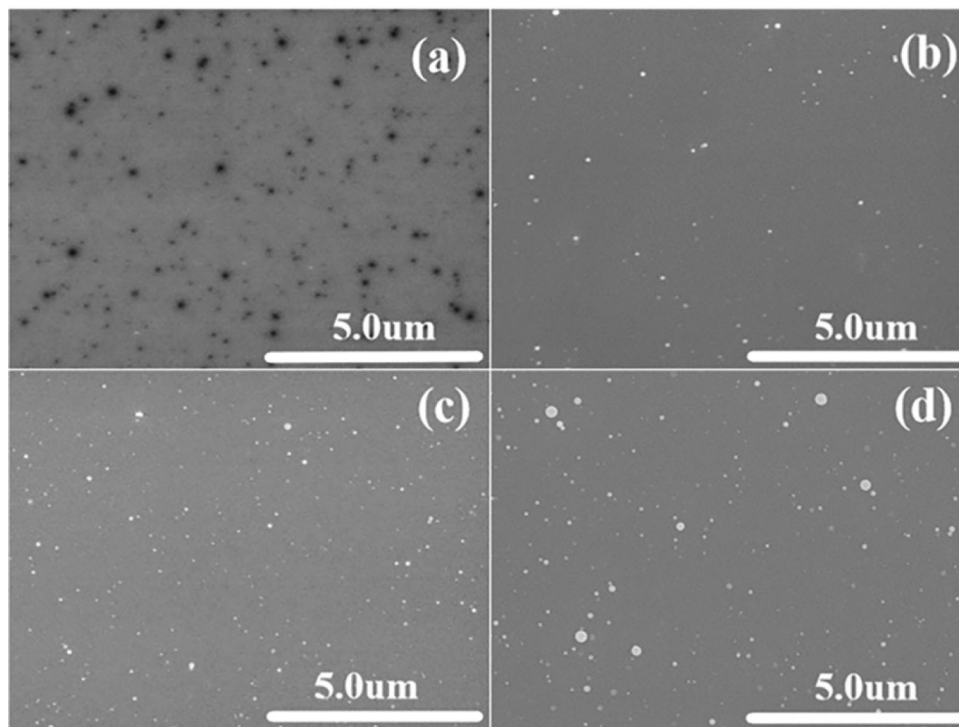


Fig. 3 SEM images of MoS₂ films prepared with laser pulse energy of 25.5 mJ/cm², laser pulse frequency of 2 Hz, and different laser pulses: **a** 400 pulses, **b** 1200 pulses, **c** 3600 pulses, and **d** 7200 pulses

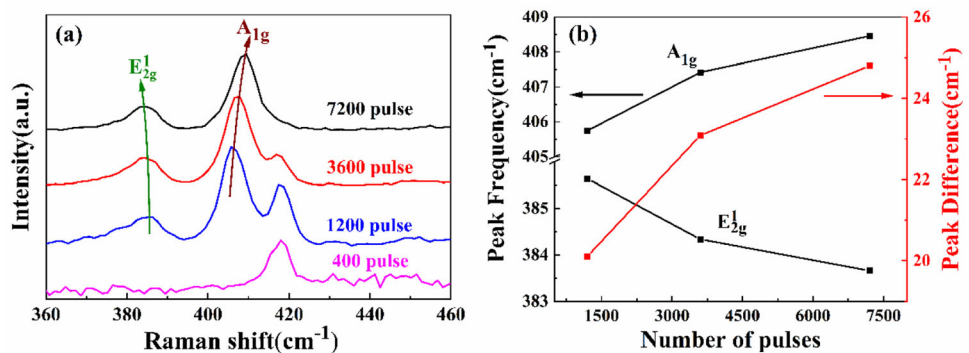


Raman spectroscopy has been used to characterize and identify the number of layers and crystalline quality of the grown thin films [26]. The measurements were done at different locations across samples in order to estimate the uniformity of the grown

films. The peak frequencies are constant at these locations for given laser parameters, confirming the thickness uniformity of MoS₂ layers over a larger area. The peaks of prominent E1 2 g (382 cm⁻¹) and A_{1g} (407 cm⁻¹) can indicate the crystalline layered

structures of MoS₂ thin films. The full width at half maximum (FWHM) of the E1 2g peak used as an indicator for crystalline quality [27]. Figure 4a shows typical Raman spectra for the different numbers of layers due to different pulses. Only the characteristic peak of sapphire substrate for 400 pulses is observed. The characteristic peak of MoS₂ has not been observed, which indicates that the MoS₂ thin film has not been formed on the substrate. As the pulse numbers increase to 1200, E1 2g and A_{1g} peaks appear in the spectrum, which can be judged that the MoS₂ thin film has been deposited. The frequency of the E1 2g peak indicates the vibration of sulfur atoms in the horizontal plane. The frequency of the A_{1g} peak indicates the vibration of sulfur atoms in the vertical plane. With the decrease of the MoS₂ layers number, the E1 2g peak will have a red shift and the A_{1g} peak will have a blue shift. When the MoS₂ film becomes monolayer, the E1 2g peak will move to around 385 cm⁻¹. As shown in Fig. 4b, the E1 2g peak frequency decreases and the A_{1g} peak frequency increases with increasing the number of laser pulses, representing the increasing of MoS₂ layers. The peak difference ($\Delta\omega$) between the two peaks, increasing with the increase of film thickness, can be used to identify the number of layers in MoS₂ thin films. The $\Delta\omega$ values are 18, 21, 23, and 24 cm⁻¹ for 1–4 layers MoS₂, respectively [28]. As shown in Fig. 4b, the $\Delta\omega$ values are 19.56, 23.35, and 24.48 cm⁻¹ at 1200, 3600, and 7200 laser pulses, respectively, which correspond to the thickness of monolayer, 2–3 layer, and multilayer. It suggests that the number of laser pulses has a small effect on the crystal quality of the MoS₂ film when it exceeds a certain value.

Fig. 4 **a** Raman spectra measurements of MoS₂ films with laser pulse energy of 25.5 mJ/cm², laser pulse frequency of 2 Hz, and different number of laser pulses. **b** The peak difference $\Delta\omega$ with different laser pulses



3.3 Effect of pulse energy density on MoS₂ thin films

Figure 5 shows the SEM images of the MoS₂ films deposited with laser pulse frequency of 10 Hz, 7200 pulses and different laser pulse energy density of 6.5, 9, 11.5, and 13 mJ/cm². Many black spots are observed on the surface of the film with a pulse energy density of 6.5 mJ/cm². The low pulse energy density is insufficient to excite massive amounts of plume plasma, which leads to the uneven surface of the growing thin film. As the pulse energy density increased to 9 mJ/cm², the black spots disappeared which shows that the thin films become homogeneous. When the pulse energy density is in the range between 9 and 13 mJ/cm², the white particles become smaller with higher energy density. Because the particles of the plume plasma suffer more intense bombardment by energy density increase, the size of the particles decrease significantly.

In Fig. 6a, the Raman spectrum indicates that the peaks of E1 2g and A_{1g} increase with pulse energy density increase; meanwhile, the characteristic peaks value of aluminum trioxide decreases. The $\Delta\omega$ increases with the pulse energy density increase, as shown in Fig. 6b. Therefore, the thickness of MoS₂ thin film can increase with the pulse energy density increase. The FWHM of E1 2g characteristic peak value changes irregularly from 8.39 to 8.75 cm⁻¹, indicating that when the pulse energy density exceeds a certain value it has a small influence on the crystalline quality of the thin films.

3.4 Effect of pulse frequency on MoS₂ thin films

The SEM images of thin films deposited with laser pulse energy of 25.5 mJ/cm², 7200 pulses and

Fig. 5 SEM images of MoS₂ films prepared with laser pulse frequency of 10 Hz, 7200 pulses and different laser pulse energy density: **a** 6.5 mJ/cm², **b** 9.0 mJ/cm², **c** 11.5 mJ/cm², and **d** 13.5 mJ/cm²

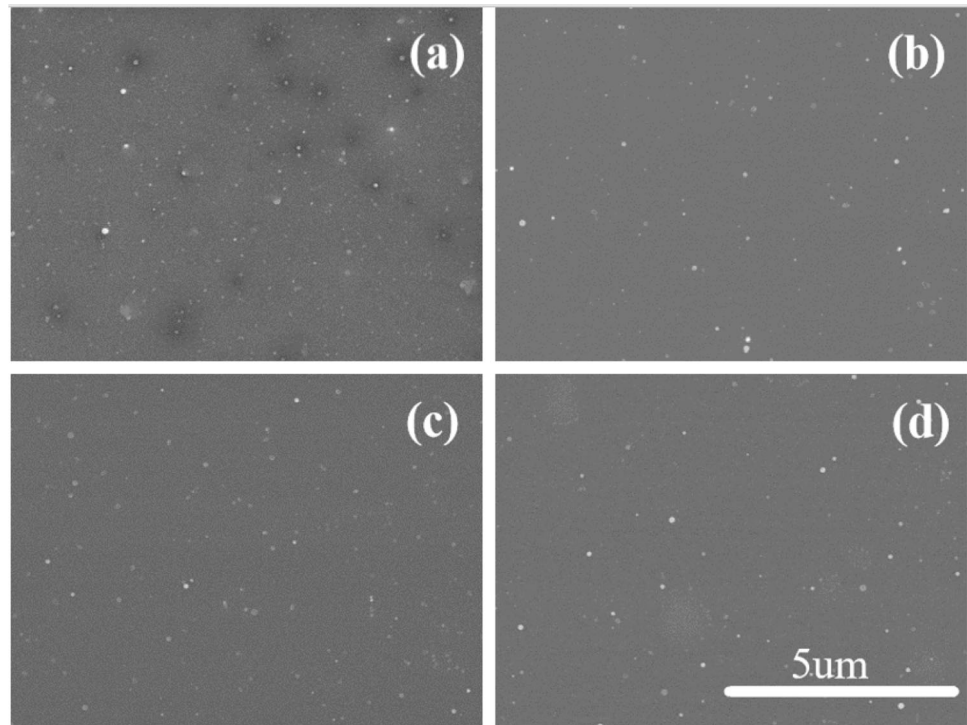
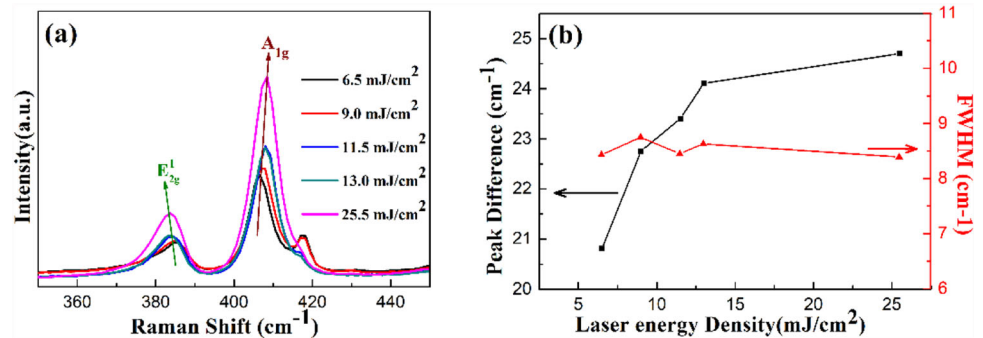


Fig. 6 a Raman spectra measurements of MoS₂ films with laser pulse frequency of 10 Hz, 7200 pulses and different laser pulse energy density. **b** Full width half maximum and peak difference with different laser pulse energy density



different laser pulse frequency of 2, 4, 6, 8, and 10 Hz are shown in Fig. 7. With the increase of pulse frequency, the size of white particles on the surface of the thin films becomes smaller, because the size of particles in the plume plasma is reduced by collisions between particles. Figure 7f illustrates particles of plume plasma collision process. Firstly, the particles of adjacent plume plasma collide with each other more intensively with the frequency increase. Secondly, the rebound particles on the substrate collide with the previously deposited particles. These collisions make the particles of plume plasma deposited on the substrates smaller.

Figure 8a shows typical Raman spectra for the films grown with different pulse frequency. The E₁ 2g and A₁g characteristic peaks of the films basically

coincide, indicating that the laser pulse frequency has a small influence on the thickness of the MoS₂ film. The FWHM of E₁ 2g peaks are found to be in the range of 7.5–9.0 cm⁻¹, consistent with the chemically exfoliated flakes (typically ~ 8 cm⁻¹) [20]. With pulse frequency increasing, the FWHM values first decrease and then increase, as shown in Fig. 8b. When the pulse frequency is 6 Hz, the value of the FWHM is minimum. Therefore the best pulse frequency of depositing high-quality MoS₂ films is 6 Hz. The crystalline quality depends on the matching of the deposition rate and the diffusion and transfer rate of particles of plume plasma on the substrate. The time of interaction between the plume plasma and substrate becomes shorter when the pulse frequency increases. If the pulse frequency is too high, over-

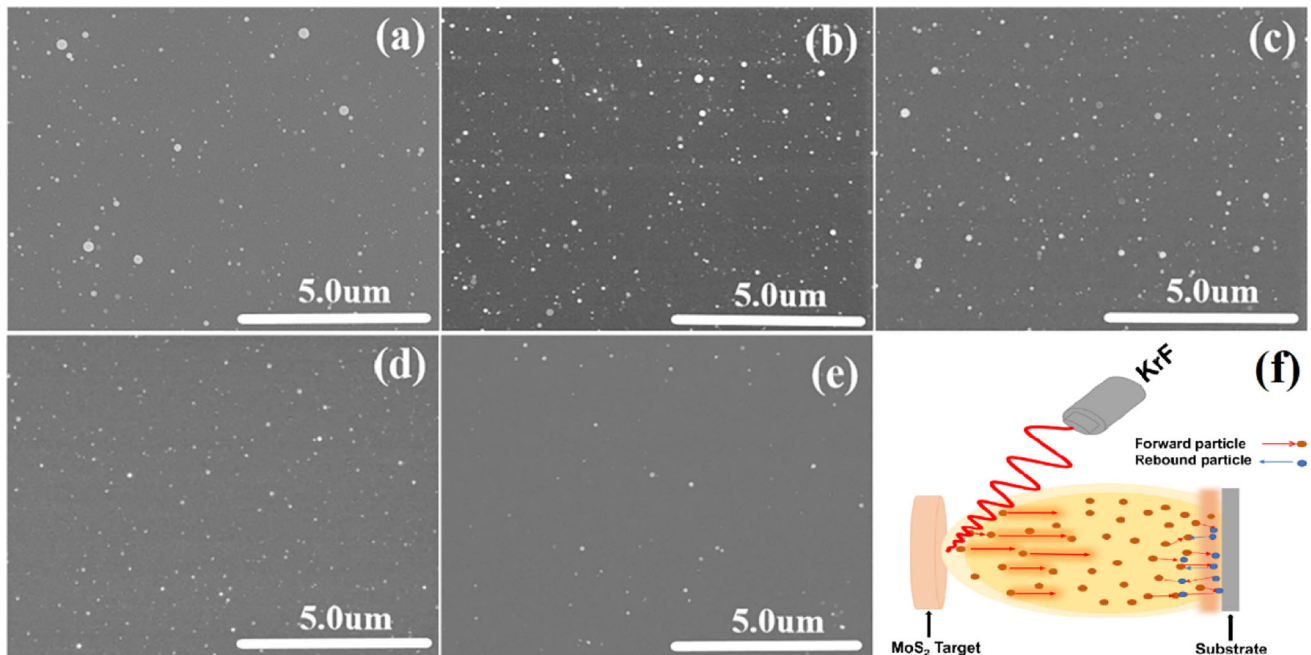
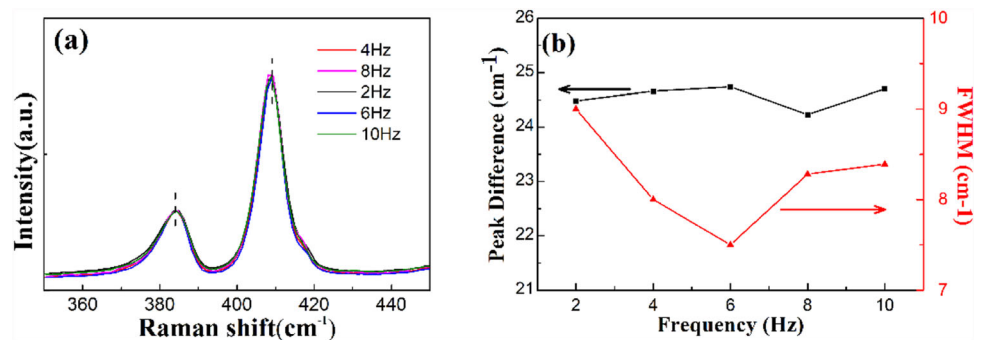


Fig. 7 SEM images of MoS₂ films prepared with laser pulse energy of 25.5 mJ/cm², 7200 pulses and different laser pulse frequency: **a** 2 Hz, **b** 4 Hz, **c** 6 Hz, **d** 8 Hz, and **e** 10 Hz.

f Schematic diagram of particles of plume plasma collision process of MoS₂ films prepared by PLD

Fig. 8 a Raman spectra measurements of MoS₂ films with laser pulse energy of 25.5 mJ/cm², 7200 pulses and different laser pulse frequency. **b** Full width half maximum and peak difference with different laser pulse frequency

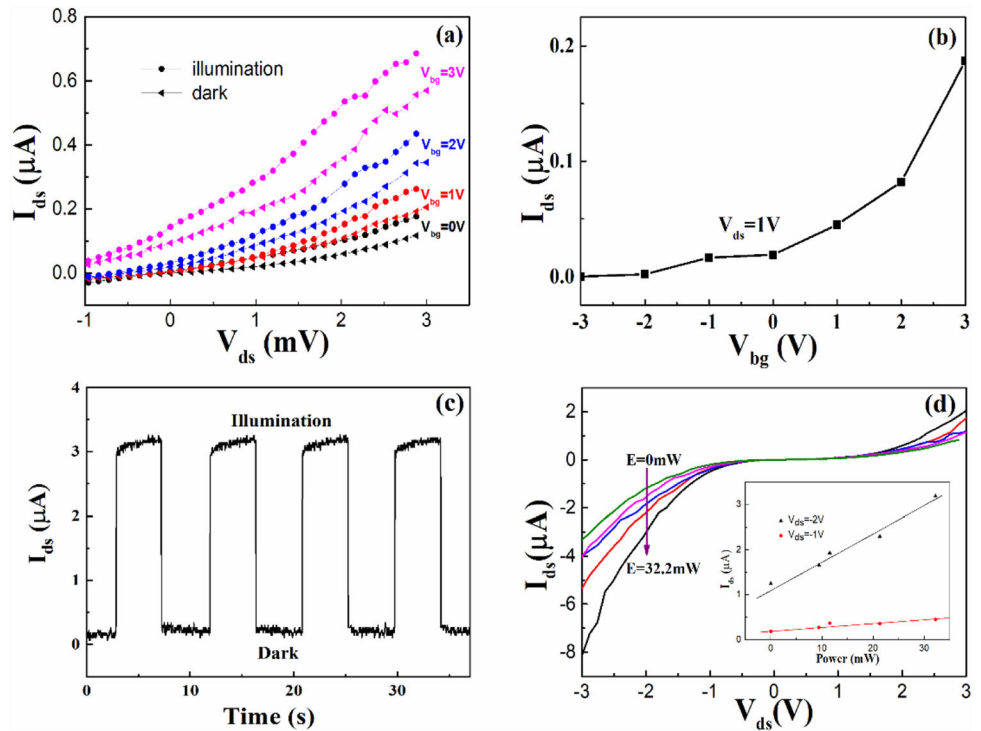


rapid deposition rate of particles of plume plasma on the substrate will lead to high nucleation density of MoS₂. The particle has not enough time to diffuse and migrate to the equilibrium position, causing poor crystalline quality of the thin film. However, if the pulse frequency is too low, low nucleation density will not promote uniform growth of the thin film, resulting in high internal stress and poor crystalline quality of the film. Based on the above study, we found that the crystalline quality of the thin film is the best with pulse frequency of 6 Hz, but the surface white particles of the thin film are the least with pulse frequency of 10 Hz.

3.5 Performance test of molybdenum disulfide FETs

To investigate the electric properties of the MoS₂ thin film, back-gated FETs were fabricated based on MoS₂ thin films, as shown in inset of Fig. 9b. The PLD parameters of MoS₂ thin film used for back-gated FET are laser pulse energy of 25.5 mJ/cm², laser pulse frequency of 6 Hz, and 7200 pulses and substrate temperature of 700 °C. The FETs take MoS₂ as channel material, metal Ag as electrode material, and the SiO₂ film as gate dielectric layer on silicon substrate. In Fig. 9a, the relationship between drain current (I_{ds}) and drain voltage (V_{ds}) at different back-gated voltage (V_g) was investigated. The recorded $I_{ds} - V_g$

Fig. 9 **a** The I – V characteristics of the MoS₂ FET in dark and illumination at different back-gated voltage. **b** Transfer characteristic of the MoS₂ FET, the inset shows SEM image of the MoS₂ FET. **c** Switching time test of the MoS₂ back-gated FET at illumination power of 32.2 mW and $V_{ds} = -2$ V. **d** The I – V characteristics of the MoS₂ FET at $V_g = 0$ V with different illumination power from 0 mW to 32.2 mW, the inset shows the photocurrent as a function of illumination power at $V_{ds} = -1$ V, $V_{ds} = -2$ V



curve (Fig. 9b) is typical of the MoS₂ FET with an n-type channel. As an important indicator to measure the electrical performance of transistor devices, carrier mobility can be estimated based on the formula:

$$\mu = \frac{L}{W \times (\epsilon_0 \epsilon_r) \times V_{ds}} \times \frac{dI_s}{dV_g}$$

where μ is carrier mobility, L is the channel length, W is the channel width, ϵ_0 is 8.854×10^{-12} F/m, ϵ_r is 3.9, d is the thickness of SiO₂ (320 nm), and V_{ds} in our experiment is 1 V. The value of dI_{ds}/dV_g can be obtained from Fig. 9b. The mobility of the FETs calculated is $4.63 \text{ cm}^2\text{V}^{-1}\text{S}^{-1}$, and the value is similar to other multilayer back-gated MoS₂ FETs prepared by CVD [29]. Electrode contact and impurities introduced in the fabrication process are the main reasons for the decrease of carrier mobility.

Because of the special band gap, MoS₂ has great potential in the application of photodetectors (PD). We tested the photosensitivity of MoS₂ back-gated FETs, the transfer characteristic curves under illumination conditions compared to dark curves are shown in Fig. 9a. I_{ds} of the sample under illumination is higher than that in dark conditions. The illumination source is xenon lamp. As shown in Fig. 9c, the switching time of the MoS₂ back-gated FET is approximately 50 ms at illumination power of 32.2

mW and drain voltage of -2 V. As shown in Fig. 9d, the current increases significantly by the incident optical power of the illumination source increase. It is indicated that MoS₂ generates photogenerated carriers under the illumination, and the MoS₂ back-gated FETs have good photosensitive properties. A linear relationship between light intensity and current can be observed, when the source-drain voltage (V_{ds}) is -1 V and -2 V (see inset in Fig. 9d). The responsivity (R) is a common technical indicator of photodetectors and can be calculated based on the formula:

$$R = \frac{(I_p - I_d)}{P_{in} \cdot A_{PD}/A_0}$$

where I_p is the current under illumination, I_d is the dark current, $|I_p - I_d| = I_{ph}$ is the photocurrent defined as the absolute change in the device current upon illumination, P_{in} is the incident light power, A_0 is the laser spot area, A_{PD} is the PD area, and A_{PD}/A_0 is a scaling factor that takes into account the fact that only a fraction of optical power impinges on the PD. The responsivity of the MoS₂ back-gated FET is approximately 0.06 AW^{-1} at V_{ds} of -2 V.

4 Conclusion

In summary, the effects of varying the laser pulse parameters on the thickness, surface morphology, and crystalline quality of the MoS₂ films fabricated by PLD were investigated. The pulses number and energy density affect surface morphology and thickness of the films. The thickness of the film is increased with pulse number and energy density increase, and the white particles on the surface decrease accordingly. The crystalline quality of the films, which mainly depends on pulse frequency, is best with pulse frequency of 6 Hz, because of the matching of the deposition rate and the diffusion and transfer rate of particles of plume plasma on the substrate. However, the number and size of white particles on the surface are inversely proportional to the pulse frequency. Finally, we have fabricated MoS₂-based FETs showing good transport characteristics with carrier mobility of 4.63 cm² V⁻¹ S⁻¹ and exhibiting excellent photosensitivity with a light responsiveness of about 0.06 AW⁻¹ at V_{ds} of -2 V. The experiment results show that the back-gated FETs based on MoS₂ thin films prepared by PLD possess potential application for photodetectors.

Acknowledgements

This work was supported by the Research Foundation for Youth Scholars of Beijing Technology and Business University (PXM2019_014213_000007).

References

- V.N. Kotov, B. Uchoa, V.M. Pereira, F. Guinea, A.H. CastroNeto, Electron-electron interactions in graphene: current status and perspectives. *Rev. Mod. Phys.* **84**, 1067 (2012)
- A. Splendiani, L. Sun, Y. Zhang, T. Li, J. Kim, Emerging photoluminescence in monolayer MoS₂. *Nano Lett.* **10**(4), 1271–1275 (2010)
- K.F. Mak, C. Lee, J. Hone, J. Shan, T.F. Heinz, Atomically thin MoS₂: a new direct-gap semiconductor. *Phys. Rev. Lett.* **105**, 136805 (2010)
- X. Xu, W. Yao, D. Xiao, T.F. Heinz, Spin and pseudospins in layered transition metal dichalcogenides. *Nat. Phys.* **10**, 343–350 (2014)
- F. Bonaccorso, Z. Sun, T. Hasan, A.C. Ferrari, Graphene photonics and optoelectronics. *Nat. Photon.* **4**, 611–622 (2010)
- A.N. Grigorenko, M. Polini, K.S. Novoselov, Graphene plasmonics. *Nat. Photon.* **6**, 749–758 (2012)
- F. Akbar, M. Kolaoudou, S. Larimian, B. Radfar, H.H. Radamson, Graphene synthesis, characterization and its applications in nanophotonics, nanoelectronics, and nanosensing. *J. Mater. Sci.: Mater. Electron.* **26**, 4347–4379 (2015)
- B. Radisavljevic, A. Radenovic, J. Brivio, V. Giacometti, A. Kis, Single-layer MoS₂ transistors. *Nat. Nanotechnol.* **6**, 147 (2011)
- W. Choi, M.Y. Cho, A. Konar, J.H. Lee, G.B. Cha, S.C. Hong, High-detectivity multilayer MoS₂ phototransistors with spectral response from ultraviolet to infrared. *Adv. Mater.* **24**(43), 5832 (2012)
- E. Singh, K.S. Kim, G.Y. Yeom, H.S. Nalwa, Atomically thin-layered molybdenum disulfide MoS₂ for bulk-heterojunction solar cells. *ACS Appl. Mater. Interfaces.* **9**(4), 3223–3245 (2017)
- A. Smolyanitsky, B.I. Yakobson, T.A. Wassenaar, E. Pau-lechka, K. Kroenlein, A MoS₂-based capacitive displacement sensor for DNA sequencing. *ACS Nano* **10**(9), 9009–9016 (2016)
- I. Jahangir, G. Koley, M.V.S. Chandrashekhara, Richardson constant and electrostatics in transfer-free CVD grown few-layer MoS₂ graphene barristor with Schottky barrier modulation > 0.6 eV. *Appl. Phys. Lett.* **110**(18), 182108 (2017)
- D.D. Fazio, I. Goykhman, M. Bruna, A. Eiden, A.C. Ferrari, High responsivity, large-area graphene/MoS₂ flexible photodetectors. *ACS Nano* **10**(9), 8252 (2015)
- H. Li, Z. Yin, Q. He, G. Lu, Fabrication of single- and multilayer MoS₂ film-based field-effect transistors for sensing NO at room temperature. *Small* **8**(1), 63–67 (2012)
- M.I. Serna, S.H. Yoo, S. Moreno, Large-area deposition of MoS₂ by pulsed laser deposition with in situ thickness control. *ACS Nano* **10**, 6054 (2016)
- C.R. Serrao, A.M. Diamond, S.L. Hsu, L. You, S. Gadgil, J. Clarkson, Highly crystalline MoS₂ thin films grown by pulsed laser deposition. *Appl. Phys. Lett.* **106**(5), 052101 (2015)
- A. Goswami, P. Dhandaria, S. Pal, R. McGee, F. Khan, Z. Antic, R. Gaikwad, K. Prashanthi, T. Thundat, Effect of interface on mid-infrared photothermal response of MoS₂ thin film grown by pulsed laser deposition. *Nano Res.* **10**, 3571–3584 (2017)
- U.P. Rathod, J.K. Jha, A.A. Voevodin, N.D. Shepherd, A photoelectron study of annealing induced changes to work-function and majority carrier type in pulsed laser deposited few layer WS₂ films. *J. Mater. Sci.: Mater. Electron.* **29**, 20051–20056 (2018)

19. Y.T. Ho, C.H. Ma, T.T. Luong, L.L. Wei, T.C. Yen, Layered MoS₂ grown on c-sapphire by pulsed laser deposition. *Phys. Status Solidi (RRL)* **9**(3), 187–191 (2015)
20. A. Barvat, N. Prakash, B. Satpati, S.S. Singha, G. Kumar, D.K. Singh, Emerging photoluminescence from bilayer large-area 2D MoS₂ films grown by pulsed laser deposition on different substrates. *J. Appl. Phys.* **122**, 015304 (2017)
21. M.I. Serna, S. Moreno, M. Higgins, H. Choi, M. Minary-Jolandan, M.A. Quevedo-Lopez, Growth parameter enhancement for MoS₂ thin films synthesized by pulsed laser deposition. *Phys. Status Solidi C* **13**, 848–854 (2016)
22. Y.K. Lin, R.S. Chen, T.C. Chou, Y.H. Lee, Y.F. Chen, K.H. Chen, L.C. Chen, Thickness-dependent binding energy shift in few-layer MoS₂ grown by chemical vapor deposition. *ACS Appl. Mater. Interfaces.* **8**(34), 22637 (2016)
23. G. Eda, H. Yamaguchi, D. Voiry, T. Fujita, M. Chen, M. Chhowalla, Photoluminescence from chemically exfoliated MoS₂. *Nano Lett.* **11**(12), 5111–5116 (2011)
24. M.Z. Xie, J.Y. Zhou, H. Ji, Y. Ye, X. Wang, K. Jiang, L.Y. Shang, Z.G. Hu, J.H. Chu, Annealing effects on sulfur vacancies and electronic transport of MoS₂ films grown by pulsed-laser deposition. *Appl. Phys. Lett.* **115**, 121901 (2019)
25. V.Y. Fominski, R.I. Romanov, D.V. Fominski, P.S. Dzhumaev, I.A. Troyan, Normal and grazing incidence pulsed laser deposition of nanostructured MoS_x hydrogen evolution catalysts from a MoS₂ target. *Opt. Laser Technol.* **102**, 74–84 (2018)
26. Y. Liu, H. Nan, X. Wu, W. Pan, Z. Ni, Layer-by-layer thinning of MoS₂ by plasma. *ACS Nano* **7**(5), 4202 (2013)
27. Y. Yu, C. Li, Y. Liu, L. Su, Y. Zhang, L. Cao, Controlled scalable synthesis of uniform, high-quality monolayer and few-layer MoS₂ films. *Sci Rep* **3**, 1866 (2013)
28. S.L. Li, H. Miyazaki, H. Song, H. Kuramochi, S. Nakaharai, K. Tsukagoshi, Quantitative raman spectrum and reliable thickness identification for atomic layers on insulating substrates. *ACS Nano* **6**(8), 7381 (2012)
29. J. Zhang, H. Yu, W. Chen, X. Tian, D. Liu, M. Cheng, Scalable growth of high-quality polycrystalline MoS₂ monolayers on SiO₂ with tunable grain sizes. *ACS Nano* **8**(6), 6024–6030 (2014)

Publisher's Note Springer Nature remains neutral with regard to jurisdictional claims in published maps and institutional affiliations.